Electron-Transfer Pathways in Dynamic Processes: Cl_2 on K

L. Hellberg, J. Strömquist, B. Kasemo, and B. I. Lundqvist
Department of Applied Physics, Chalmers University of Technology and Göteborg University, S-412 96 Göteborg, Sweden
(Received 16 December 1994)

Detailed observation and analysis of exoelectron emission from velocity-selected Cl_2 molecules impinging on a K surface imply a reaction pathway, where surface harpooning, surface-modified electron affinities, molecular dissociation dynamics, and Auger neutralization are key ingredients. To account for the data, a model proposed by Nørskov, Newns, and Lundqvist is extended to include the nonadiabatic electron affinity of Cl_2 and an explicit treatment of the Cl_2 dissociation trajectories for different incident orientations.

PACS numbers: 79.20.Nc, 34.70.+e, 79.20.Rf, 82.65.My

This Letter addresses three general phenomena in physics, chemistry, and biology, namely charge transfer, dissociation dynamics of molecules, and nonadiabatic electronic processes. An ideal model case, where these phenomena are intimately interrelated, is explored experimentally and theoretically.

The model system is a beam of Cl_2 molecules with varying kinetic energy (0.08–0.68 eV) impinging on a potassium surface. The final result of the exothermic reaction is Cl atoms or rather Cl^- ions, embedded in the potassium surface. In the course of Cl_2 dissociation and Cl^- embedding, two consecutive electron transfers occur and energetic electronic excitations are created, causing emission of photons, (exo)electrons, and Cl^- ions. The experiment produces new data on the velocity-dependent intensity and energy distribution of the exoelectrons. We develop a conceptually simple model that significantly extends the surface chemiluminescence model of Nørskov, Newns, and Lundqvist (NNL) [1]. The analysis identifies a highly excited hole (electron vacancy) as an intermediate state and key details about the Cl_2 dissociation. It should have general bearings on charge transfer and dissociation dynamics, especially in molecule-surface encounters.

Emission of charged particles (e^-, ions) [2–8] and light (surface chemiluminescence) [4,7,8] during gas adsorption at metal surfaces is generally attributed to nonadiabatic charge transfer processes. The NNL mechanism [1] successfully accounts for the spectral trends of surface chemiluminescence from the reaction of halogens with sodium [7]. In an expanded version it describes also exoelectron emission in an O_2/metal reaction [5]. Its essential ingredients are (i) electron transfer (harpooning [9–11]) to the image-shifted affinity level of the incident molecule, followed by (ii) image acceleration, to produce a velocity gain, and (iii) a second, strongly nonadiabatic electron transfer to an image-shifted atomic affinity level (excited hole). By changing the substrate from Na to K the different roles of resonance and Auger electron transfer are illustrated [8]. Böttcher and co-workers [6] have elucidated the electron emission from O_2/alkali metal reactions by several experiments and theoretical analysis. They employ and further develop the model to explain, e.g., the oxygen-coverage dependence of the electron emission. O_2 and O, more complex than halogens, undergo a number of charge transfer reactions before electron emission. On metallic Li the sequence is $O_2 \rightarrow O_2^- \rightarrow O_2^{2-} \rightarrow O^- + O^-$, $O^- \rightarrow O^{2-}$ + exoelectron. Acceleration of the molecular ion by image attraction is found vital for the nonadiabaticity, as in the NNL model.

In all the work above adiabatic electron affinities have been used, while charge transfer to a molecule involves both electronic and nuclear degrees of freedom, implying harpooning closer to the surface than in the adiabatic case, with a concomitant loss of the important image acceleration. We show here that use of the correct nonadiabatic molecular electron affinity leads to a qualitatively new picture of the electron emission and surface chemiluminescence, where dissociation dynamics and molecular orientation at the harpooning distance are important ingredients, not treated earlier.

The experiments are performed in a UHV chamber at 10^{-10} torr base pressure by sending a beam of Cl_2 molecules onto a K surface at 130 K. Approximately 1.6×10^{13} Cl_2 molecules per second impinge normally on a 0.55 cm^2 area. The K surface is prepared by depositing an $\approx$50 nm thick film on a Si substrate. Auger electron spectroscopy is used to check the surface cleanliness. The Cl_2 beam of variable energy is formed by an alumina nozzle, followed by three differentially pumped beam-forming stages. The beam energy is varied by He seeding [12], and velocity controlled by a double-chopper arrangement. The total electron yield is measured as the negative-particle current leaving the sample. Negative-ion emission (Cl^-) is negligible compared with electrons. The energy distribution $N(E)$ of the electrons is measured by a planar three-grid analyzer. Complementary information is obtained by a modified mass spectrometer, detecting negative ions, by an optical system, detecting photons, and by work-function measurements. All presented data concern the first molecules incident on the clean metal surface, i.e., before there is any appreciable Cl coverage.

The main experimental results are shown in Figs. 1 and 2. The electron emission yield depends strongly on the velocity v of the incident molecules perpendicular to the

 0031-9007/95/74(23)/4742(4)$06.00

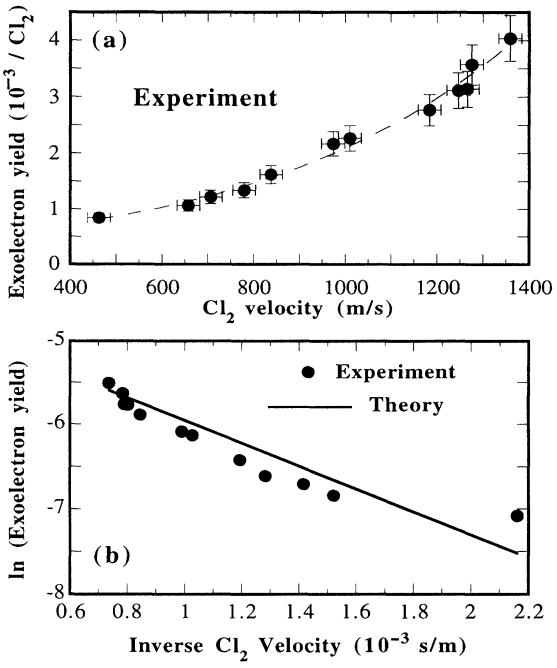

FIG. 1. (a) Measured exoelectron current as a function of the Cl_2 velocity. The dashed line is a guide to the eye only. (b) Theoretical and experimental dependences of the current as functions of the inverse Cl_2 velocity.

surface (Fig. 1). $N(E)$ also depends on v (Fig. 2). The curves are normalized to a common maximum intensity. There is a small but significant shift to higher energies with increasing velocity. The maximum lies at about 1 eV kinetic energy, and the high-energy cutoff at 2–2.5 eV for the highest velocity. (The energy scale was calibrated by the photoemission spectrum produced by the Hg line at 254 nm. The energy uncertainty is about 0.5 eV.)

To account for the data, trajectory calculations have been performed for Cl_2 molecules approaching the surface with different velocities and orientations, using gas-

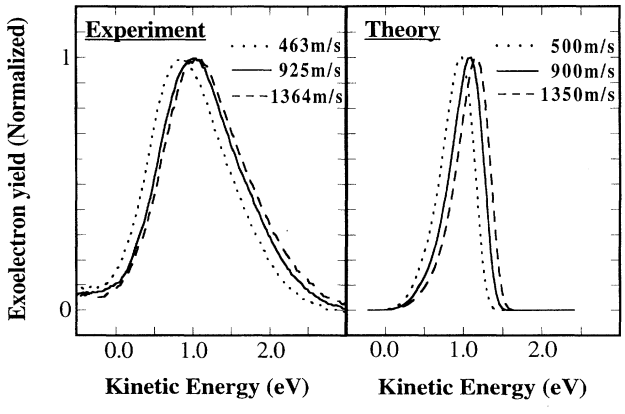

FIG. 2. The (a) measured and (b) calculated kinetic energy distribution $N(E)$ of the emitted Auger electrons at three different Cl_2 velocities v.

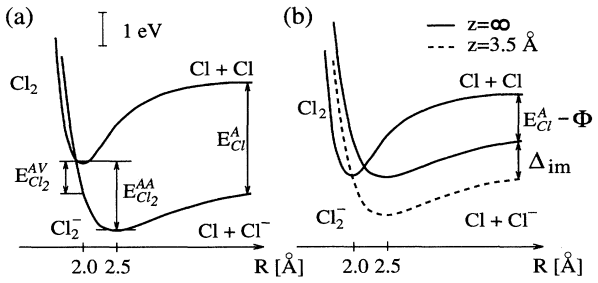

FIG. 3. Molecular potential energy curves (PEC) of free Cl_2 and Cl_2^- as functions of internuclear distance R with the electron applied from (a) the vacuum level and (b) the Fermi level of potassium. The dashed curve shows how the Cl_2^- PEC is image shifted $\Delta_{im} = 1.3$ eV at 3.5 Å from the surface.

phase intramolecular Morse potentials [13] (Fig. 3) and ion-surface image forces. Our model has four key steps [numbered (1)–(4) in Fig. 4]: (1) Around 4 Å from the surface, measured from the jellium edge, a harpooning electron is sent from the K surface to the antibonding orbital of Cl_2. The Cl_2^- ion immediately dissociates or forms a temporary negative-ion state. As the Cl and Cl^- fragments of the dissociating molecular ion separate, the empty $3p$ level of the Cl atom is rapidly shifted downwards, producing an excited hole. This hole is either filled by resonant electron transfer from the metal (2) or survives until its affinity level E^A_{Cl} is shifted below the bottom of the K conduction band (3). It then deexcites by an Auger transition (4) or radiative decay, producing measurable electrons or surface chemiluminescence, respec-

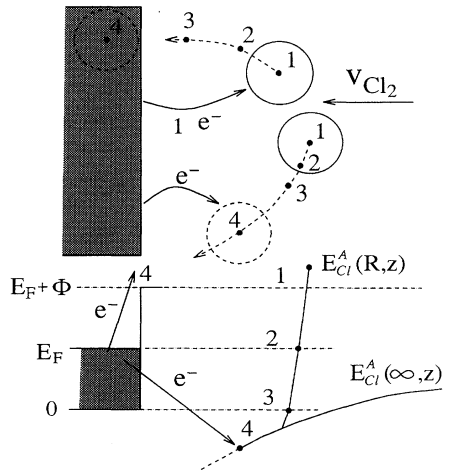

FIG. 4. Schematic picture of the model in the case of a molecule with an initial orientation of 20°. In the top part events (1)–(4) denote atomic positions and charge transfer events. In the bottom part events (1)–(4) denote the corresponding affinity level positions $E^A_{Cl}(R,z)$ of the Cl atom. For comparison the free atom affinity level is shown as $E^A_{Cl}(\infty,z)$. Event (4) is the Auger process of Cl producing the electron emission, and the Cl^- ion is already screened out by the electron gas.

tively. Electron emission requires the energy level, E^A_{Cl}, to be shifted clearly below the bottom of the conduction band, since for K the work function Φ (2.3 eV) is larger than the bandwidth (2.1 eV). The most energetic detected exoelectrons indicate an affinity level 2–2.5 eV below the band, corresponding to a hole-excitation energy of about 4.2–4.7 eV. The available reaction heat is estimated to be at least 6 eV. An intermediate state with an excitation energy close to the reaction heat has thus been identified.

We elucidate its origin by three estimates: (i) Merely shifting the free atomic affinity by the effective potential [14] gives a value of 5.8 eV, an overestimate [15]. (ii) Calculations for a Cl atom embedded with the $(2p)^6$ and $(2p)^5$ configurations, respectively, in a homogeneous electron gas with the potassium density, give a value of 4.1 eV [16]. (iii) A self-consistent calculation with Cl on a jellium surface corresponding to Na [17] places the level 2.9 eV below the band, i.e., a hole-excitation energy of 5 eV, if translated to K. In our calculations the level is placed 3 eV below the band at the jellium edge.

We now consider the probability of creating a hole with sufficient energy to produce electron emission and explain the observed velocity dependences (Figs. 1 and 2).

Far away from the surface the *adiabatic* affinity level of Cl_2, $E^{AA}_{Cl_2} = 24$ eV, lies 0.1 eV below the Fermi level, E_F, of potassium [Fig. 3(b)], and electron transfer is energetically allowed at any distance. However, $E^{AA}_{Cl_2}$ corresponds to a transition from Cl_2 to Cl_2^-, each at their equilibrium bond lengths ($R^0_{Cl_2} = 2.0$ Å and $R^0_{Cl_2^-} = 2.5$ Å, respectively), and the corresponding Franck-Condon factors are negligible. Electron transfer requires a vertical transition, but the *vertical* affinity $E^{AV}_{Cl_2}$, corresponding to Cl_2 and Cl_2^- having the same bond length $R^0_{Cl_2}$, lies 1.3 eV above E_F far away from the surface [Fig. 3(b), full curves]. Closer to the surface the image downshift Δ_{im} of the Cl_2^- potential energy curve (PEC) [dashed curve in Fig. 3(b)] makes the two PECs cross successively closer to the Cl_2 minimum. When the crossing point has reached the minimum at $z = 3.5$ Å, $E^{AV}_{Cl_2}$ is in resonance with electron states at E_F and an electron can now tunnel to Cl_2. This produces a compressed Cl_2^- ion on the repulsive part of its PEC, which causes separation. A higher initial velocity makes this harpooning event occur closer to the surface and places the $Cl_2 \rightarrow Cl_2^-$ transition higher up on the Cl_2^- repulsive wall, which favors immediate dissociation. Conversely, a lower velocity causes earlier harpooning and favors formation of a temporarily trapped negative-ion state. (In the gas phase electron attachment to Cl_2 inevitably induces dissociation [Fig. 3(a)].) The calculations described below show (i) that the *primary* cause of the increase in exoelectron yield is the larger fraction of directly dissociating molecules at higher velocities, and (ii) that the fraction of directly dissociating molecules and thus the exoelectron yield increase with v as $\exp(-\text{const}/v)$.

During the initial about 50 fs of the Cl_2^- dissociation a second electron transfer to Cl is not possible due to the strong Coulomb repulsion from Cl^-. As Cl and Cl^- separate, and Cl^- simultaneously approaches the surface, the Coulomb repulsion diminishes due to the increased separation and the screening of Cl^- by the electron gas. Consequently, $E^A_{Cl}(R, z)$ rapidly shifts down from far above E_F [(1) in Fig. 4], through the band states, where resonance filling might occur, to below the K conduction band, where it approaches $E^A_{Cl}(\infty, z)$. The concerted dissociation motion (along R) and the z motion makes $E^A_{Cl}(R, z)$ shift through the K band at $z \geq 3.5$ Å in typically 30 fs, which is fast enough and sufficiently far from the surface that the hole with a fairly high probability survives resonance filling. (Note that for the molecular orientation in Fig. 4 the $3p$ hole shifts from above Φ to below the band with very little change in the z coordinate.)

The probability of exoelectron emission depends strongly on the orientation of the incident Cl_2 molecule. With the molecular axis parallel to the surface the probability is very low (10^{-4}–10^{-5}), since resonance filling of E^A_{Cl} is then effective. With an oblique orientation in the range 10°–30°, as in Fig. 4, the probability is much higher ($\sim 10^{-1}$). This is due to the temporal retardation (along the R coordinate) of the Cl atom and, in particular, the faster approach of the Cl^- to the surface caused by the repulsion within the Cl_2^- molecular ion.

We now consider the shape of $N(E)$ and its shift with changing velocity. They are explained as follows: When $E^A_{Cl}(R, z)$ reaches the threshold for electron emission at Φ below E_F, the Auger rate is still small and the phase space (energy and angular) for electron emission is small. As the Cl atom comes closer to the surface the Auger decay rate increases rapidly, as does the excitation energy (Fig. 4). A higher incident v means that the Cl atom, on the average, comes a little closer to the surface before the second electron transfer occurs, giving a larger average excitation energy. This redistributes holes from lower to higher energy and explains the shift of $N(E)$ with v.

In the calculations the energy positions, widths, and occupancies of the two one-electron states E^A_{Cl} and $E^A_{Cl_2}$ are followed along the nuclear trajectories, with the following input: The $Cl_2 \rightarrow Cl_2^-$ transition is treated by coupling the Cl_2 and Cl_2^- vibronic states as in gas-phase $M + I_2$ collisions, where M is a metal atom [18]. For $E^A_{Cl_2}$ the Franck-Condon weighted (nonadiabatic) electron affinity is used. The charge transfer to the molecule by resonance tunneling is calculated in the semiclassical approximation [19] in the case of no back donation from the molecule (temperature $T = 0$). The electron population $n_{Cl_2^-}$ is given by

$$\frac{d}{dt} n_{Cl_2^-}(t) = \tau^{-1}_{res} f(E^A_{Cl_2}(t))[1 - n_{Cl_2^-}(t)], \qquad (1)$$

where τ^{-1}_{res} is the resonance filling rate and f is the Fermi function. Guided by calculations for Cl/Al [20] and Cl/K [21] we approximate $\hbar\tau^{-1}_{res} = 2\Delta_0 \exp(-\alpha_{res} z)\rho(E)/\rho(E_F)$, where $\Delta_0 = 20$ eV, $\alpha_{res} = 1.7$ Å^{-1}, and ρ is the bulk density of states. Once the first electron transfer has occurred (Fig. 4), dissociation begins and the value

of $E^A_{Cl}(R,z)$ is determined by the image charges and the real charge on Cl^-. As the E^A_{Cl} level shifts down rapidly through the K band it is subject to resonance filling described by Eq. (1), now applied to Cl.

The Auger transitions, only effective in a limited range of z values, are described by an exponential Auger rate τ^{-1}_{Aug} and calculated with an equation similar to Eq. (1). Calculations suggest [22] that α_{Aug} in $\tau^{-1}_{Aug} = A\exp(-\alpha_{Aug}z)$ is about $2\alpha_{res}$. The absolute value of A is not known. Production of exoelectrons with kinetic energies ≥ 1 eV requires $A \leq 10^{18}\ s^{-1}$. The $N(E)$ curves in Fig. 2(b) are obtained by projecting dn_{Cl^-}/dz onto $E^A_{Cl}(\infty,z)$. Good agreement is obtained when $\alpha_{Aug} = 3.8\ Å^{-1}$ and $A = 2 \times 10^{17}\ s^{-1}$. (Comparable A and α_{Aug} were used in Refs. [23,24].) The absolute yield of the emitted electrons [Fig. 1(b)] was calculated assuming that 10% of the internally produced Auger electrons can escape and be detected externally [23].

In summary, we have measured new electron emission data and developed a simple coherent picture of Cl_2 dissociation on a potassium surface, initiated by harpooning. Our model attributes the velocity dependence of the exoelectron yield to the larger fraction of spontaneously dissociating Cl_2 at higher velocity. It explains the shift to higher energies of the electron energy distribution with increasing incident velocity as a "velocity-memory effect," making the Auger transitions occur closer to the surface and with higher energy at higher velocities. Compared to Nørskov, Newns, and Lundqvist [1] and later developments of that model [6,25], the present treatment has several decisively new features, modifying even the qualitative picture of how the excited state causing electron emission is created. First, consideration of both electronic and vibrational overlap drastically reduces the harpooning distance where the first electron transfer occurs. As a consequence, much less image acceleration of the molecular ion occurs. Instead the nonadiabaticity responsible for electron and photon emission is connected with the dissociation dynamics including steric effects, which must be treated explicitly.

Support from the NFR (E-EG 03106-345) and TFR (92-9511) are gratefully acknowledged.

[1] J. K. Nørskov, D. M. Newns, and B. I. Lundqvist, Surf. Sci. **80**, 179 (1979).
[2] J. J. Thomson, Philos. Mag. **36**, 308 (1905).
[3] L. Himmel and P. Kelly, Comments Solid State Phys. **7**, 81 (1976).
[4] B. Kasemo, Phys. Rev. Lett. **32**, 1114 (1974).
[5] B. Kasemo *et al.*, Surf. Sci. **89**, 554 (1979).
[6] A. Böttcher *et al.*, Phys. Rev. Lett. **65**, 2035 (1990); K. Hermann *et al.*, Surf. Sci. **313**, L806 (1994); T. Greber, Chem. Phys. Lett. **222**, 292 (1994).
[7] B. Kasemo and L. Walldén, Surf. Sci. **53**, 393 (1975).
[8] D. Andersson, B. Kasemo, and L. Walldén, Surf. Sci. **152/153**, 576 (1985).
[9] M. Polanyi, *Atomic Reactions* (Williams and Norgate, London, 1932).
[10] J. L. Magee, J. Chem. Phys. **8**, 687 (1940).
[11] J. W. Gadzuk, Comments At. Mol. Phys. **16**, 219 (1985).
[12] G. Scoles, *Atomic and Molecular Beam Methods* (Oxford University Press, New York and Oxford, 1988).
[13] P. Davidovits and D. L. McFadden, *Alkali Halide Vapors: Structure, Spectra, and Reaction Dynamics* (Academic Press, New York, 1979), p. 429.
[14] N. D. Lang and A. R. Williams, Phys. Rev. B **18**, 616 (1978).
[15] O. Gunnarsson, H. Hjelmberg, and J. K. Nørskov, Phys. Scr. **22**, 165 (1980).
[16] J. Hartford (private communication).
[17] N. D. Lang, J. K. Nørskov, and B. I. Lundqvist, Phys. Scr. **34**, 77 (1986).
[18] E. A. Gislason and J. G. Sachs, J. Chem. Phys. **62**, 2678 (1975).
[19] D. C. Langreth and P. Nordlander, Phys. Rev. B **43**, 2541 (1991).
[20] P. Nordlander, Phys. Rev. B **46**, 2584 (1992). Γ for Cl on Al.
[21] P. Nordlander (private communication). Γ for Cl on K.
[22] T. Fondén and A. Zwartkruis, Surf. Sci. **269/270**, 601 (1992).
[23] H. D. Hagstrum, Phys. Rev. **96**, 325 (1954); **96**, 336 (1954).
[24] R. E. Walkup, P. Avouris, and N. D. Lang, Phys. Rev. Lett. **63**, 1972 (1989).
[25] E. B. Deblasi Bourdon and R. H. Prince, Surf. Sci. **144**, 591 (1984).